JOURNAL OF VIROLOGY, July 2003, p. 7477–7485 Vol. 77, No. 13
0022-538X/03/$08.00+0 DOI: 10.1128/JVI.77.13.7477–7485.2003
Copyright © 2003, American Society for Microbiology. All Rights Reserved.

Dynamics of Viral and Proviral Loads of Feline Immunodeficiency Virus within the Feline Central Nervous System during the Acute Phase following Intravenous Infection

G. Ryan,[1] D. Klein,[2] E. Knapp,[2] M. J. Hosie,[3] T. Grimes,[4] M. J. E. M. F. Mabruk,[5] O. Jarrett,[3] and J. J. Callanan[1,6]*

Department of Veterinary Pathology[1] and Small Animal Clinical Studies,[4] Faculty of Veterinary Medicine, and Conway Institute of Biomolecular and Biomedical Research,[6] University College Dublin, Belfield, Dublin 4, and Department of Pathology, Royal College of Surgeons in Ireland, Beaumont Hospital, Dublin 9,[5] Ireland; Institute of Virology, University of Veterinary Medicine, Vienna, Austria[2]; and Department of Veterinary Pathology, University of Glasgow, Bearsden, Glasgow, Scotland[3]

Received 10 September 2002/Accepted 12 April 2003

Animal models of human immunodeficiency virus 1, such as feline immunodeficiency virus (FIV), provide the opportunities to dissect the mechanisms of early interactions of the virus with the central nervous system (CNS). The aims of the present study were to evaluate viral loads within CNS, cerebrospinal fluid (CSF), ocular fluid, and the plasma of cats in the first 23 weeks after intravenous inoculation with FIV_{GL8}. Proviral loads were also determined within peripheral blood mononuclear cells (PBMCs) and brain tissue. In this acute phase of infection, virus entered the brain in the majority of animals. Virus distribution was initially in a random fashion, with more diffuse brain involvement as infection progressed. Virus in the CSF was predictive of brain parenchymal infection. While the peak of virus production in blood coincided with proliferation within brain, more sustained production appeared to continue in brain tissue. In contrast, proviral loads in the brain decreased to undetectable levels in the presence of a strengthening PBMC load. A final observation in this study was that there was no direct correlation between viral loads in regions of brain or ocular tissue and the presence of histopathology.

Infection of domestic cats with the lentivirus feline immunodeficiency virus (FIV) may result in a range of clinical signs related to an underlying state of immunodeficiency (48, 65). FIV shares many features with human immunodeficiency virus type 1 (HIV-1) (48, 49, 67), particularly in causing lymphoid system pathology (13, 14), immune dysfunction (27, 64), and high-grade B-cell lymphomas (15). Furthermore, FIV and HIV share a common mechanism of infection via the CXCR4 receptor molecule (66). The trademark five clinical stages of HIV-1 infection are mirrored in FIV-infected cats, beginning with an acute flu-like illness shortly after infection and ending with conditions associated with severe immunodeficiency (19, 39, 50).

FIV, like HIV-1, infects the central nervous system (CNS) and is associated with neuropathology in natural and experimental infections (25, 26, 38, 40, 55–58). Early after intravenous inoculation, virus can be recovered from primary cultures of the cerebral cortex, caudate nucleus, midbrain, cerebellum, caudal brain stem, and cerebrospinal fluid (CSF) (25, 56, 67). FIV-infected cells have been detected in the brain as early as 7 days following intravenous challenge (7), and in vitro studies demonstrate that FIV preferentially infects astrocytes and brain macrophages, with low affinity for brain endothelial cells (26).

HIV-1 infection is associated with neuropathology in the early and AIDS stages of infection (12). There are, however, limited opportunities to examine early stages of HIV infection (5), and the spectrum of neuropathology in HIV-1 infection is naturally biased towards the end stages of disease, which are complicated by opportunistic infections and intensive therapies (12). The time and manner in which HIV-1 gains entry into and subsequently spreads within the microglial cells is poorly understood due to limited opportunities to examine the brain in the presymptomatic stages of infection (1). It is generally accepted that the characterization of these early stages can most readily be achieved through the use of animal models (12, 52). The lentivirus infections of macaques and domestic cats are excellent models for HIV infection of humans (28, 47), with early infection of the brain documented in both animal groups (7, 8, 16, 58). The dissection of the early virus-host interactions in such models may assist the development of therapies to modulate lentivirally induced CNS infection and help to investigate to what extent CNS tissue harbors reservoirs of latently infected cells, which are an important challenge when formulating lentiviral therapeutic strategies (6, 59).

While FIV viral and proviral loads within peripheral blood have been determined by several PCR-based methods (10, 41, 43, 44, 54, 58, 62), viral loads within FIV-, simian immunodeficiency virus (SIV)-, or HIV-infected brains have been determined by visual quantification of infected cells using in situ hybridization or immunocytochemical techniques (2, 7, 8) and to a limited extent by PCR technologies (18, 58). Taqman, fluorogenic, real-time PCR has recently been applied in the determination of FIV, SIV, and HIV viral and proviral loads within peripheral blood mononuclear cells (PBMCs) and var-

* Corresponding author. Mailing address: Department of Veterinary Pathology, Faculty of Veterinary Medicine, University College Dublin, Belfield, Dublin 4, Ireland. Phone: 35317166152. Fax: 35317166157. E-mail: sean.callanan@ucd.ie.

TABLE 1. FIV *gag*-specific primers and probe used in FIV fluorogenic Taqman real-time PCR assay[a]

Primer or probe	Sequence (5′ to 3′)	Fragment size (bp)
Forward primer, FIV 1360f	GCA GAA GCA AGA TTT GCA CCA	
Reverse primer, FIV1437r	TAT GGC GGC CAA TTT TCC T	78
Probe, FIV1416p	FAM-TGC CTC AAG ATA CCA TGC TCT ACA CTG CA-TAMRA	
Forward primer, rRNA343f	CCA TCG AAC GTC TGC CCT A	
Reverse primer, RRNA409r	TCA CCC GTG GTC ACC ATG	67
Probe, RRNA370p	FAM-CGA TGG TGG TCG CCG TGC CTA-TAMRA	

[a] Cell number estimation was done using primers and probe targeting the 18S ribosomal DNA genes.

ious tissues (9, 30, 35, 41, 43–45, 60, 61). This technique is an improvement on previous quantitative or semiquantitative PCR-based methods. Studies correlating plasma, CSF, and brain viral and proviral loads have been documented to a limited degree for HIV and SIV infection and in particular have focused on asymptomatic or end stages of disease (20, 63, 68). More recently, evaluations of the acute phase of FIV and SIV infections have been reported (10, 18). Plasma and CSF viremias have been monitored during the first 18 weeks following FIV infection (10), and using an accelerated model of SIV-induced encephalitis, monitoring of CNS viral DNA and RNA together with CSF and plasma RNA was achieved over an 8-week period (18). Similarly to the latter study, the present study addresses the dynamics of viral and proviral loads during the acute phase of infection. This period is particularly important, since it represents one window of time in which virus is believed to enter the brain (29).

The aims of the present study were to determine viral loads within compartments of the brain at sequential time points in early FIV_{GL8} infection by Taqman, fluorogenic, real-time PCR methods. Specifically, this study was designed to determine if FIV enters brain tissue following intravenous infection, over what time frame infection occurs, and whether virus distribution is in a uniform pattern. Second, the study evaluated virus dynamics in the early stages of infection by determining the viral concentrations within the brain and correlating them to plasma and CSF concentrations, to brain tissue and PBMC proviral loads, and to brain histopathology.

MATERIALS AND METHODS

Study design. Twelve (six male and six female), 16- to 20-week-old specific-pathogen-free cats were inoculated intravenously with 2,000 infectious-unit doses of the FIV_{GL8} isolate (31). Eight (four male and four female) 16- to 20-week-old specific-pathogen-free cats were maintained separately as controls. Five cats (three infected and two controls) were sacrificed at 1, 4, 10, and 23 weeks after infection. Blood samples were taken at 1, 4, 8, 10, and 23 weeks after infection. Blood was stored in EDTA (1.3 mg/ml) (LIP Ltd., Galway, Ireland) at 4°C until nucleic acid was extracted. At 4 weeks after infection, all remaining infected animals were confirmed to be seropositive by immunofluorescence (32). Animal experimental procedures were performed under an approved license. FIV_{GL8} is a primary isolate that has been passaged minimally in feline T cells (32). In contrast to the prototypic Petaluma strain isolated (FIVPET), FIV_{GL8} has a limited in vivo cell host range that does not extend to the CrFK cell line (33), and it is virulent in vivo, leading to high viral loads in plasma (35).

Before necropsy, animals were anaesthetized with 10 mg of ketamine hydrochloride (Vetalar; Pharmacia & Upjohn, Corby, United Kingdom)/kg of body weight and 3 mg of Xylazine (Bayer, Bury St. Edmunds, United Kingdom)/kg, and after intracardiac exsanguination, were sacrificed by administering 150 mg of pentobarbitone sodium (Euthatal; Rhone Merieux, Harlow, United Kingdom)/kg by the intracardiac route. Plasma was stored at −80°C, and whole blood was maintained at 4°C.

At necropsy, CSF was obtained from the foramen magnum and immediately stored at −80°C. A midsagittal sectioning of the brain was performed. One portion was fixed in neutral buffered formalin, and the second portion was separated into cerebrum, cerebellum, and brain stem, which were snap-frozen in liquid nitrogen and stored at −80°C. Ocular fluid was sampled from the anterior chamber of the right eye and stored at −80°C. Both eyes were then fixed in neutral buffered formalin.

Following fixation in formalin, sections of cerebrum, cerebellum, midbrain, pons, medulla, spinal cord, and eye were paraffin embedded, cut at 4 μm, and stained with hematoxylin and eosin. Utilizing a cryostat, cross sections of frozen brain, weighing 30 mg, were obtained from similar portions of the cerebrum and cerebellum and from the pons region of the brain stem.

Nucleic acid extraction. To determine FIV viral loads, RNA was extracted from 30 mg of brain tissue using an RNeasy mini kit (Qiagen, Hilden, Germany). Viral RNA was extracted from plasma, CSF, and ocular fluid using a QIAamp Viral RNA mini kit (Qiagen). DNA was extracted from 30-mg tissue samples from the cerebrum, cerebellum, and brain stem using a QIAamp DNA kit (Qiagen) and from 200 μl of whole blood using QIAamp blood DNA mini kits (Qiagen). The extracted DNA and RNA samples were eluted with 30 μl of water, from which 5 μl was used in the Taqman real-time PCRs.

Real-time PCR. The 25-μl real-time PCR mixtures contained 10 mM Tris (pH 8.3), 50 mM KCl, 3 mM $MgCl_2$, 200 uM deoxynucleotide triphosphates, 300 nM (each) primer, 200 nM fluorogenic probe, 1.25 U of *Taq* DNA polymerase per reaction, and 5 μl of diluted template or genomic standard. After initial denaturation for 2 min at 95°C, amplification was performed with 45 cycles of 95°C for 15 s and 60°C for 1 min followed by a holding step of 25°C. Amplification, data acquisition and data analysis were carried out in an ABI Prism 7700 sequence detector (Applied Biosystems, Foster City, Calif.). Data were analyzed with Sequence Detection Software (version 1.6.3; Applied Biosystems). The primers and probes used are described in Table 1.

Real-time RT-PCR. The 25-μl RT-PCR mixtures contained 10 μl of AMV/Tfl 5× reaction buffer (Access RT-PCR system; Promega, Mannheim, Germany), 3 mM $MgSO_4$, 200 μM dATP, dCTP, dGTP, and dTTP, 300 nM (each) primer, 200 nM fluorogenic probe, 5 U of avian myeloblastosis virus reverse transcriptase, 5 U of Tfl DNA polymerase and 5 μl of the sample or RNA standard. After a reverse-transcription step of 45 min at 48°C followed by a denaturation step (2 min at 95°C), amplification was performed with 45 cycles of 15 s at 95°C and 60 s at 60°C. Reverse transcription and amplification were performed using an ABI Prism 7700 sequence detection system (Applied Biosystems). The detected fluorescence signals are analyzed using the Sequence Detection Software version 1.6.3 (Applied Biosystems). The primers and probes used are described in Table 1.

RESULTS

To evaluate the FIV_{GL8} intravenous infection model, the study had first to establish if in fact the time course of the infection did include the acute phase characterized by a transient increase in viral plasma loads coupled with a follow-on period of undetectable to minimal peripheral virus production. The purpose of the present study was not to undertake a detailed frequent sequential analysis of viral loads but rather to relate loads observed in plasma to those in the CNS at the selected times of necropsy. However, it was clear that following intravenous FIV_{GL8} infection, highest viral loads of the order of between 1×10^2 and 1×10^4 copies per ml of plasma were documented at 4 and 10 weeks following infection and by 23

TABLE 2. Viral loads in the brain, CSF, ocular fluid, and plasma and proviral loads in the brain and PBMCs from all 12 FIV_{GL8}-infected cats at four time points over the 23-week course of infection[a]

Week p.i., animal, or sample type	Viral load[b]	PV load (copies/10^6 cells)	Path[c]	Week p.i., animal, or sample type	Viral load[b]	PV load (copies/10^6 cells)	Path[c]
Week 1				Week 10			
Animal 1				Animal 11			
Cerebrum	0	0	−	Cerebrum	3,074	476	++
Cerebellum	*	0	−	Cerebellum	5,336	130	+
Brain stem	152	0	−	Brain stem	2,012,080	586	+
CSF	0			CSF	6,837		
Ocular	0		−	Ocular	34		+
Plasma/PBMC	0	5		Plasma/PBMC	1,151	87,169	
Animal 2				Animal 12			
Cerebrum	0	0	−	Cerebrum	0	0	+
Cerebellum	*	0	−	Cerebellum	0	0	+
Brain stem	0	0	−	Brain stem	4,630	0	−
CSF	0			CSF	105		
Ocular	0		−	Ocular	0		+
Plasma/PBMC	0	0		Plasma/PBMC	496	1,774	
Animal 3				Animal 13			
Cerebrum	0	0	−	Cerebrum	0	0	+
Cerebellum	*	0	−	Cerebellum	0	0	−
Brain stem	0	0	−	Brain stem	51,210	109	−
CSF	0			CSF	61		
Ocular	0		−	Ocular	0		+
Plasma/PBMC	0	0		Plasma/PBMC	374	1,895	
Week 4				Week 23			
Animal 6				Animal 16			
Cerebrum	29,780	418	−	Cerebrum	202	0	++
Cerebellum	392	4	−	Cerebellum	200	0	+
Brain stem	82	116	−	Brain stem	316	0	−
CSF	400			CSF	151		
Ocular	42		+	Ocular	0		++
Plasma/PBMC	10,292	425		Plasma/PBMC	0	3,350	
Animal 7				Animal 17			
Cerebrum	0	7	−	Cerebrum	0	0	+
Cerebellum	0	0	+	Cerebellum	0	0	−
Brain stem	0	244	−	Brain stem	0	0	−
CSF	37			CSF	0		
Ocular	24		+	Ocular	0		+
Plasma/PBMC	77	384		Plasma/PBMC	33	1,636	
Animal 8				Animal 18			
Cerebrum	0	24	−	Cerebrum	456	0	+
Cerebellum	0	0	−	Cerebellum	162	0	−
Brain stem	0	0	−	Brain stem	70	0	−
CSF	40			CSF	22		
Ocular	0		+	Ocular	0		+
Plasma/PBMC	187	344		Plasma/PBMC	0	5,668	

[a] Asterisk, not done; −, absent; +, mild; ++, moderate.
[b] Viral load is expressed as number of copies/gram for cerebrum, cerebellum, and brain stem and as number of copies/milliliter for CSF, ocular, and plasma/PBMC.
[c] Path, presence of CNS or ocular histopathology.

weeks after infection loads had dramatically decreased or were at undetectable levels (Table 2 and Fig. 1a) in animals that had seroconverted. While, in contrast to previous FIV studies (22, 36, 51, 62), such peak loads in the acute phase of infection were relatively small, previous studies would support the presence of greater concentrations in between the relatively long sampling points which were undertaken in this study. Such concentrations were also comparable with those of HIV and SIV infections (23, 31, 53). A marked reduction in viral loads followed the initial viremia and was in contrast to observations in previous FIV, SIV, and HIV studies, where loads stabilized at between 2×10^3 and 7×10^5 copies/ml (18, 23, 31, 51, 53, 62).

In the same time frame in the present study, PBMC proviral loads concentrations, estimated at 1, 4, 8, 10, and 23 weeks after infection, increased (Table 3, Fig. 2a). For this calculation, two different real-time PCR assays were used: the FIV proviral copy number was calculated targeting the FIV *gag* gene (43), and the cell number was estimated targeting the 18s ribosomal DNA genes (42). Low proviral copy numbers (5 to 65 copies/10^6 cells) were initially detected in 2 of 12 infected

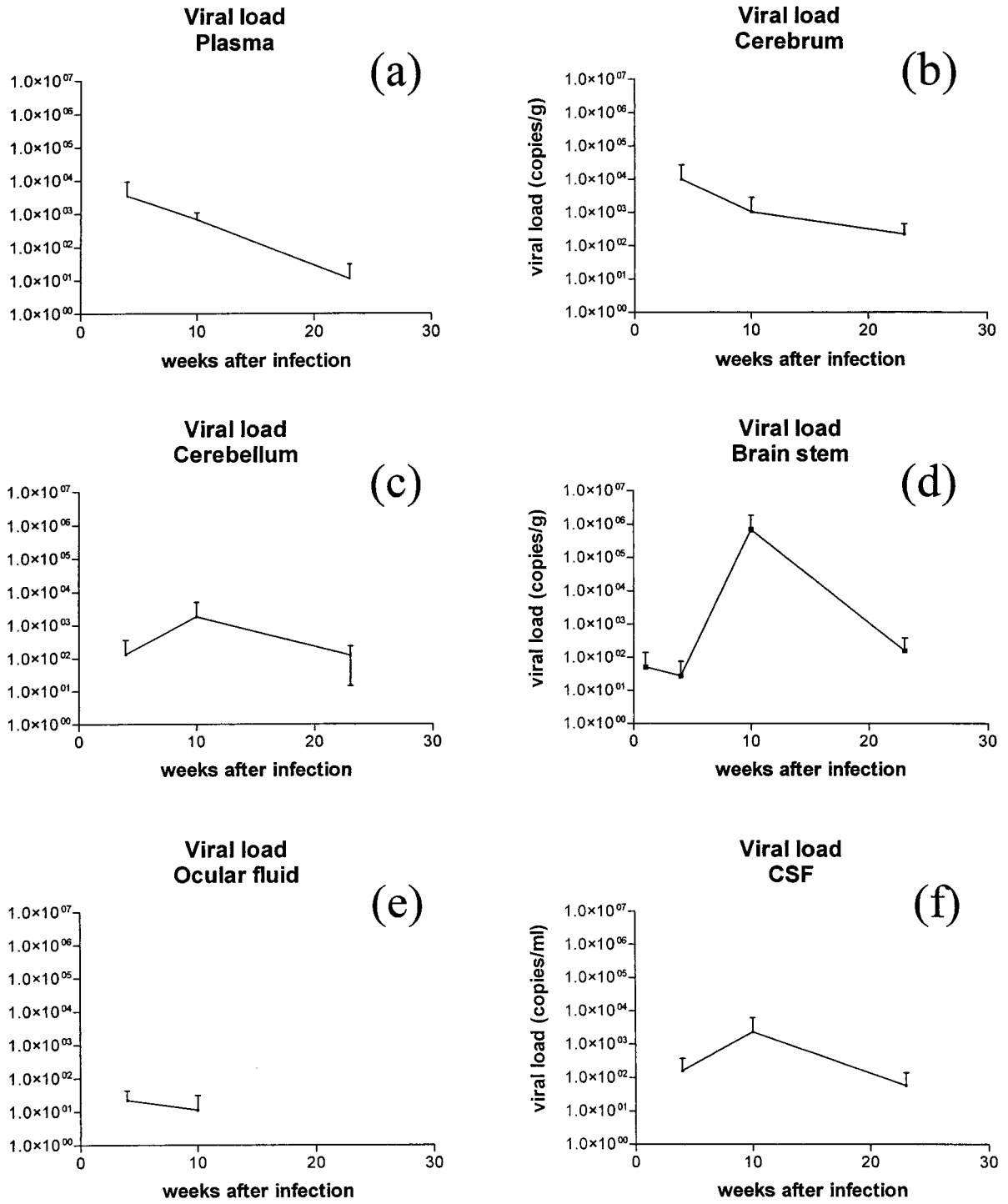

FIG. 1. Mean viral loads in cats challenged with FIV_{GL8} (copies per gram of tissue or copies per milliliter of fluid) detected by Taqman real-time RT-PCR during the 23-week postinfection period.

animals at week 1 after infection. Proviral loads between 107 and 1,254 copies/10^6 cells were observed in all nine infected animals sampled at 4 weeks after infection. The greatest concentrations were of the order of between 1,500 copies/10^6 cells and 87,169 copies/10^6 cells, noted from 8 weeks postinfection onwards until the completion of the study at 23 weeks after infection. The magnitude of and individual variation between proviral loads were in agreement with results in other FIV, SIV, and HIV studies (4, 21, 31, 35, 36, 58).

Viral and proviral loads in the cerebrum, cerebellum, and brain stem were estimated at the time of necropsy (Table 2; Fig. 1b, c, and d; Fig. 2b, c, and d). At each time, loads were quite variable between individual animals and between regions of the brain. By week 1 after infection, virus was detected in the

TABLE 3. Proviral loads in PBMCs (copies of FIV/10^6 cells) from cats challenged with FIV_{GL8} during the 23-week postinfection period

Cat no.	Proviral load (no. of copies/10^6 cells) at no. of weeks postinfection[a]				
	1	4	8	10	23
1	5				
2	0				
3	0				
6	65	425			
7	0	384			
8	0	344			
11	0	1,209	13,908	87,169	
12	0	506	1,574	1,774	
13	0	107	863	1,895	
16	0	542	2,554	*	3,350
17	0	295	2,280	*	1,636
18	0	1,254	2,466	*	5,668

[a] Asterisk, no data was obtained.

brain stem region of one animal (animal no. 1; 152 copies/g). At this time point no provirus was detected. By week 4, while only the animal with the highest serum viral load (no. 6) had detectable viral RNA in all three brain regions examined (80 copies/g to nearly 3×10^4 copies/g), all three animals had proviral loads (between 4 and 418 copies/10^6 cells). By week 10, all three animals had detectable viral RNA in brain tissue. The brain stem consistently contained high viral RNA loads, but the concentrations were quite variable (4×10^3, 5×10^4, and 2×10^6 copies/g). Proviral concentrations of between 109 and 586 copies/10^6 cells were observed in two animals only. By week 23, two of the three infected animals had detectable virus in all compartments of the brain examined. However, no provirus was detected in the brain tissue of any of the three animals examined. There was no clear pattern in either the regional distribution or in the magnitude of the concentrations of virus or provirus within the brain. Of the three regions examined for 12 animals, 14 regions had detectable virus and 10 regions had detectable provirus in quantities that varied between 80 and 2×10^6 copies/g and between 4 and 586 copies/10^6 cells, respectively.

To date, there has been very little information on viral loads within the CNS in FIV infection (58). The present study strengthened the observations that for the majority of animals the acute phase of infection is a significant time in which virus invades the CNS (7, 8, 37, 58). In fact, at the last time point of the study, only one animal had no detectable virus within the CNS or CSF, which would be more suggestive of a lack of CNS infection than of a transient infection which had been cleared or reduced to undetectable concentrations. While studies using similar quantification techniques have been undertaken using the SIV model, such studies have been primarily concerned with viral loads as they related to the end stages of disease, when the animal is likely to have encephalitis (20, 68). A recent study on an accelerated model of SIV-induced encephalitis revealed CNS viral loads in all animals at 10 weeks after infection, but in contrast to the present study, loads rapidly reduced to undetectable concentrations by 3 weeks, with a resurgence of loads in selected animals by 7 weeks (18).

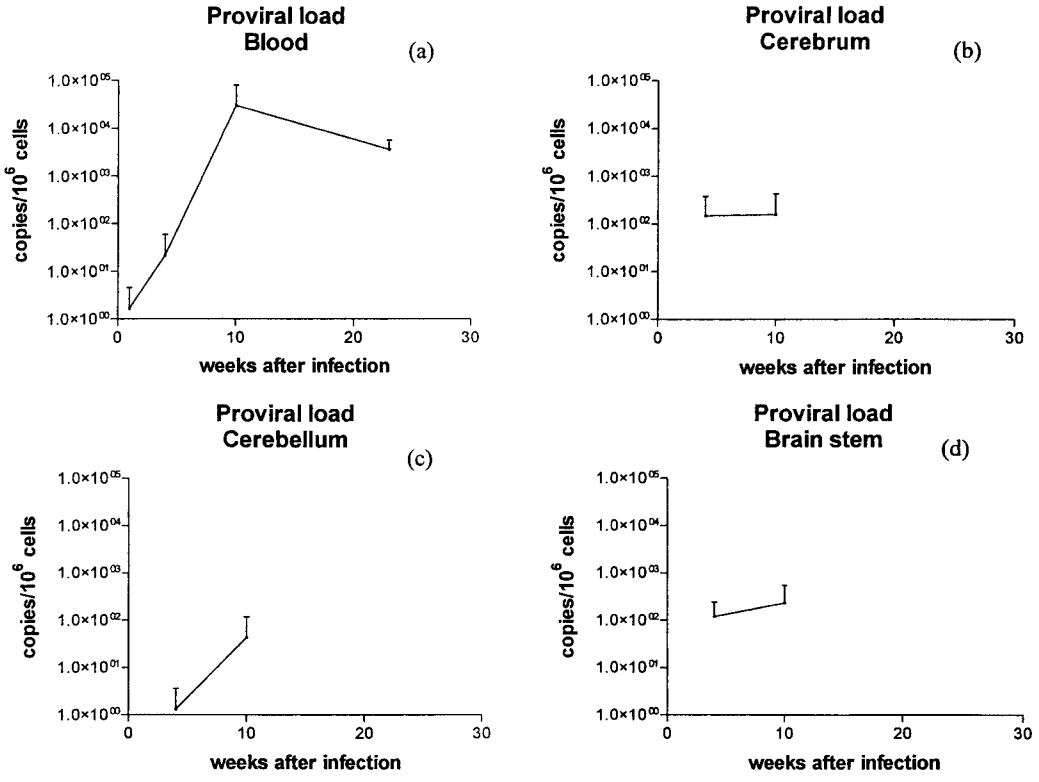

FIG. 2. Mean proviral loads (viral copies per 10^6 cells) in cats in the 23-week period following intravenous infection with FIV_{GL8}. Results are shown for PBMCs (a), cerebrum (b), cerebellum (c) and brain stem (d).

Of concern in the present study, as in other studies, has been the fact that viral and proviral loads in blood may contribute to tissue values (18, 63, 68). Some studies have overcome this problem through tissue perfusion with saline (18, 68), while others have calculated the influence based on the assumptions that between approximately 5 and 10% of tissue volume may be blood (63). To reduce, but not eliminate, the effects of blood volume, our animals were exsanguinated during the euthanasia procedure. In addition, our results in many instances would not correlate with blood contamination, particularly when brain concentrations exceed 1/10 that of plasma. Thirdly, frequently in the present study regions of the brain were devoid of detectable virus or provirus even when a viral or proviral load was detectable within the plasma or PBMCs, respectively.

The magnitude of the concentrations of FIV RNA in 14 of 33 regions of brain parenchyma examined varied between approximately 1×10^2 and 2×10^6 copies per g of brain. Since similar studies focusing on the acute phase of infection have not been undertaken with HIV, it was not possible to truly compare viral loads between lentiviral infections. However, studies by Wiley and colleagues (63) documented viral loads between 1×10^3 and 4.5×10^7 copies of RNA per gram of brain tissue in HIV-infected AIDS patients with minimal to severe neuropathological changes. In a study by Zink and colleagues (68) to induce SIV AIDS and encephalitis, greater viral concentrations of between 1.4×10^9 and 3.8×10^{10} copies per g of brain tissue were calculated for terminally ill animals. However, studies on the acute stages of infection by this group revealed that viral RNA within the CNS is rapidly downregulated, to resurge with the onset of encephalitis (18). In agreement with the work of Wiley and colleagues (63), in the present study it was clear that viral RNA was not uniformly distributed throughout the brain during initial infection. However, in animals sacrificed towards the end of the study, a more uniform distribution of virus among all brain compartments was noted. It is difficult to draw conclusions as to why FIV, like HIV, appears to proliferate in many regions of the brain independent of their connectivity. However, while the limited sampling from each region may in part contribute to such findings, Wiley and colleagues (63) observed such changes with extensive sampling and suggested that local factors and monocyte trafficking may promote viral expression. In SIV infection, regional variations in viral loads have also been documented, with cerebellar viral loads lower than cortical, midbrain, and brain stem loads but in general less variable than those documented in HIV-1 infection and in the present study (68).

As with viral loads, proviral loads also appeared to vary between compartments. It was somewhat surprising that by 23 weeks of infection provirus was not detected in the brain, although this features was also noted by Pederson and colleagues (51) following a 20-week study with both FIV-Apetaluma and FIV-Cpgammar. Such findings were in contrast those of to another FIV study, which documented proviral loads over 2-year period, although loads did decrease following acute infection and prolonged sampling times were in operation (58).

In comparing viral RNA concentrations in plasma to those of the CNS, the transient virus proliferation in plasma coincided with the onset of CNS virus proliferation, although CNS viral loads remain elevated throughout the duration of the study. Animals euthanatized between weeks 4 and 10 displayed both the greatest concentrations of viral RNA within plasma and in the brain (Fig. 1). In addition, at these time points animals 6 and 7, with the greatest concentrations of plasma viral RNA, had detectable viral RNA in all compartments of the brain examined. In contrast, by week 23, animals with undetectable plasma viral RNA continued to have detectable viral RNA in all brain compartments examined. A second contrasting feature was the trend for proviral PBMC loads to increase with progression of infection while proviral loads within the CNS were detected only in weeks 4 and 10 following infection and were absent by week 23 (Fig. 2d).

Viral loads in the CSF were determined at the time of necropsy (Table 2; Fig. 1f). Viral RNA concentrations of between 40 and 400 copies/ml were first detected at 4 weeks following infection for all three animals (Table 2; Fig. 1f). At 10 weeks, all three animals also had detectable viral RNA (60 to 6,837 copies/ml) in CSF, and the two animals at 23 weeks after infection with detectable virus in the CNS also had CSF virus at concentrations between 22 and 151 copies/ml. While portions of brain tissue varied in viral and proviral loads and frequently compartments sampled had no detectable viral RNA or provirus, CSF consistently predicted that virus or provirus would be present in at least one portion of the brain. This would suggest that within this model, CSF viral load determinations would be the best predictor of early brain infection and could be a useful tool in CNS antiviral therapy studies which may focus on the acute stage of infection. The only exception was animal 1, euthanatized within 1 week of infection, in which virus was detected in the brain stem only and not in the CSF, suggesting that in the initial weeks of infection there is a potential short lag period before virus is observed in the CSF. The viral loads observed in the present study varied between 20 and 6×10^3 copies per ml and were obtained at four time points. Thus, they were unlikely to reflect peak concentrations. Evaluations of SIV CSF viral loads in acute infection revealed peak values of the order of 1×10^4 to 1×10^6 copies per ml between 10 and 14 days after infection, followed by a slight decrease or a stabilization at these values (68). Similar concentration were noted for FIV (10). No time course studies to evaluate CSF viral loads in the acute stages of HIV infection have been undertaken due to inabilities to capture this phase; however, many studies, biased towards the latter stages of infection, have positively correlated CSF viral loads with encephalopathy and dementia (11, 17, 24, 46).

A final observation of the study was that the magnitude and distribution of histopathological changes in brain and ocular tissue did not correlate with either tissue viral or proviral loads. Histopathological findings are summarized in Table 2 and form part of a more detailed publication on the neuropathology of FIV_{GL8} (G. Ryan, M. Mabruk, T. Grimes, B. Brankin, M. Hosie, O. Jarrett, and J. Callanan, unpublished data). In brief, microscopic examination of the cerebrum, cerebellum, and brain stem (midbrain, medulla pons) revealed perivascular lymphocyte cuffing of blood vessels within the meninges covering the cerebrum, cerebellum, and brain stem within the cerebral white matter and within the choroid plexus. While lesions were initially noticed 4 weeks after infection, they were more widespread and of greatest severity at weeks 10 and 23 after infection. At these time points there was clear variation

between individuals in the severity of the microscopic changes. Ocular lesions consisted of perivascular lymphocyte accumulations within the scleral limbus and within the iris, ciliary body, and choroid. Lesions were initially noticed at 4 weeks after infection, but again they were more consistently observed, and of greatest severity, at weeks 10 and 23 postinfection.

In general the wave of viral replication within tissues preceded histopathological changes, since lesions were more prominent by weeks 10 and 23 after infection. However, a clear correlation between the concentration of virus within regions of brain and the magnitude of histopathological changes was not found. Similarly, while histopathological changes in the eye were noted in all nine animals sacrificed from week 4 onwards, virus was only detected in the ocular fluid of two animals at 4 weeks after infection and in one animal at 10 weeks (range, 24 to 42 copies per ml) (Table 2; Fig. 1e).

Both animals 11 and 16 had marked cerebral and ocular pathology. For animal 11, this coincided with markedly elevated viral loads. However, for animal 16, viral loads were considerably lower and were like those of animal 18, which had minimal pathology. Similarly, animal 6, at 4 weeks after infection, had prominent viral and proviral brain tissue loads but did not display any detectable histopathological changes in the brain. This animal did have limited ocular pathology, and virus was detected in ocular fluid. In contrast, at week 23, animal 17, while not having detectable virus in brain or ocular fluid, did have CNS and ocular histopathology changes.

Relating viral and proviral concentrations to CNS and ocular histopathology highlighted that while there was an overall trend for histopathological lesions to follow the onset of peripheral and CNS virus production, the magnitude of lesions within individual compartments of tissue did not correlate with the concentrations of virus and provirus observed in these regions. This factor, together with the observation that proviral DNA was detectable only transiently within the CNS, raises two interesting questions. Is the histopathology observed a response to viral presence in the CNS? Is viral CNS infection in the acute stages of disease a transient feature?

While many studies positively correlated viral loads with end-stage neuropathology in HIV, SIV, and FIV infections (7, 20, 29, 63, 68), the present study focused on the pathology associated with the acute phase of infection, and thus, there are few comparable studies (10, 18, 58). The lesions of meningeal, choroid plexus, and parenchymal mononuclear cell perivascular cuffing observed in the acute phase of infection are essentially features of the trafficking of mononuclear cells through the CNS, and as documented previously (7, 8, 20, 37), some of these cells are likely to be infected with virus. It is believed, however, that in HIV infection such cell accumulations are not due to localized virus production but are a reflection of a generalized systemic immune stimulation (29). This hypothesis is supported in the present study, since generalized reactive hyperplasia has been observed in association with early FIV_{GL8} infection commencing in a time frame similar to that of the onset of neuropathological lesions and the presence of perivascular mononuclear cell lesions in other organs, such as ocular tissue (13, 14). A second supporting feature was the observed trend for lesions to develop following the systemic proliferation of virus, and it would explain why animals such as animal 17, while showing no evidence of viral infection of the CNS, did show neuropathology. However, in the latter case, although unlikely, one cannot discount the possibility that virus had been in the brain earlier and had been eliminated or reduced to undetectable concentrations. Previous recent studies on the early stages of FIV infection, while not concentrating on histopathology, have documented an increased toxic activity of CSF and upregulation of CD18 in association with a decreased CSF and plasma viremia (10), while a positive correlation was noted between proviral loads and tumor necrosis factor alpha expression (58). In a comparable SIV study, histopathology was not observed in 17 of 18 macaques sequentially examined in an 8-week period following infection, although subtle immune and inflammatory changes, such as macrophage activation and the infiltration of cytotoxic lymphocytes, were noted (18).

While it is clear that FIV does ultimately cause neuropathology, it is not clear if the early observation of viral RNA in CSF and brain tissue is sustained and if this leads to the development of reservoirs of infection within the brain or this initial CNS infection is truly transient. It is well known that CSF viral loads may not necessarily reflect virus replication in the brain parenchyma but can develop as a result of virus replication in the meninges, from infected cells trafficking through the CSF, or from plasma-derived virus entering through a compromised blood-brain barrier (20, 63, 68). Similarly, it has been suggested that SIV loads in brain parenchyma may also be a reflection of transient infection by trafficking mononuclear cells (20). Studies of asymptomatic HIV-1-infected patients who die some years after seroconversion either show exceptionally low proviral loads within brain tissue, consistent with levels expected from the presence of blood vessel viral loads, or may show evidence of true low-grade infections (3, 5). With the increasing sensitivity of virus detection methods, it has been suggested that viral loads become dramatically reduced or regionalized and that the CNS functions as a reservoir for latent infection during the asymptomatic phase of infection (6, 18, 59). This obviously has major implications in the design of therapies to prevent or modify lentiviral CNS infections, since it would suggest that the acute stages of infection may be the most significant period in viral infection of the brain. Such possibilities highlight the need for an extension of the present study which would examine FIV-infected animals at frequent intervals over a longer period from the acute phase of infection and into an established asymptomatic phase. In particular, it would be desirable to perform extensive brain tissue sampling corroborated by in situ hybridization techniques in this period to further track the fate of CNS viral loads in an environment of reduced or undetectable peripheral blood loads and to monitor proviral loads in brain tissue in the presence of a strengthening PBMC proviral load.

ACKNOWLEDGMENTS

We acknowledge the technical assistance of colleagues in the Department of Veterinary Pathology, University College Dublin (S. Worrall, C. King, B. Cloak, and J. Brady) and in the University of Veterinary Medicine, Vienna, Austria.

This work was funded by a Faculty of Veterinary Medicine, University College Dublin, Research Stimulus Grant. Collaborations with the University of Veterinary Medicine, Vienna, Austria, were funded through the FAVEUR Concerted Action of the European Commission.

REFERENCES

1. **Achim, C. L., R. D. Schrier, and C. A. Wiley.** 1991. Immunopathogenesis of HIV encephalitis. Brain Pathol. **1:**177–184.
2. **Achim, C. L., R. Wang, D. K. Miners, and C. Wiley.** 1994. Brain viral burden in HIV infection. J. Neuropathol. Exp. Neurol. **53:**284–294.
3. **An, S. F., and F. Scaravilli.** 1997. Early HIV-1 infection of the central nervous system. Arch. Anat. Cytol. Pathol. **45:**94–105.
4. **Bagnarelli, P., S. Menzo, A. Manzin, M. Giacca, P. E. Varaldo, and M. Clementi.** 1991. Detection of human immunodeficiency virus type 1 genomic RNA in plasma samples by reverse-transcription polymerase chain reaction. J. Med. Virol. **34:**89–95.
5. **Bell, J. E., A. Busuttil, J. W. Iornside, S. Rebus, Y. K. Donaldson, P. Simmonds, and J. F. Peutherer.** 1993. Human immunodeficiency virus and the brain: an investigation of virus load and neuropathologic change in pre-AIDS subjects. J. Infect. Dis. **168:**818–824.
6. **Blankson, J. N., D. Persuad, and R. F. Siliciano.** 2002. The challenge of viral reservoirs in HIV-1 infection. Annu. Rev. Med. **53:**557–593.
7. **Boche, D., M. Hurtel, F. Gray, M-A. Claessens-Marie, J.-P. Ganière, L. Montagnier, and B. Hurtrel.** 1996. Virus load and neuropathology in the FIV model. J. Neurovirol. **2:**377–387.
8. **Boche, D., E. Khatissian, F. Gray, P. Falanga, L. Montagnier, and B. Hurtrel.** 1999. Viral load and neuropathology in the SIV model. J. Neurovirol. **5:**232–240.
9. **Boretti, F. S., C. M. Leutenegger, C. Mislin, R. Hofmann-Lehmann, S. Konig, M. Schroff, C. Junghans, D. Fehr, S. W. Huettner, A. Habel, J. N. Flynn, A. Aubert, N. C. Pedersen, B. Wittig, and H. Lutz.** 2000. Protection against FIV challenge infection by genetic vaccination using minimalistic DNA constructs for FIV env gene and feline IL-12 expression. AIDS **14:** 1749–1757.
10. **Bragg, D. C., L. C. Hudson, Y. H. Liang, M. B. Tompkins, A. Fernandes, and R. B. Meeker.** 2002. Choroid plexus macrophages proliferate and release toxic factors in response to feline immunodeficiency virus. J. Neurovirol. **8:**225–239.
11. **Brew, B. J., L. Pemberton, P. Cunningham, and M. G. Law.** 1997. Levels of human immunodeficiency virus type 1 RNA in cerebrospinal fluid correlate with AIDS dementia stage. J. Infect. Dis. **175:**963–966.
12. **Budka, H.** 1991. Neuropathology of human immunodeficiency virus infection. Brain Pathol. **1:**163–175.
13. **Callanan, J. J., H. Thompson, S. R. Toth, B. O'Neill, C. E. Lawrence, B. Willett, and O. Jarrett.** 1992. Clinical and pathological findings in feline immunodeficiency virus experimental infection. Vet. Immunol. Immunopathol. **35:**3–13.
14. **Callanan, J. J., P. Racz, H. Thompson, and O. Jarrett.** 1993. Morphological characterisation of lymph node changes in feline immunodeficiency virus infection as an animal model of AIDS, p. 115–136. *In* P. Racz, N. L. Letvin, and J. C. Gluckmann (ed.), Animal models of HIV infection. Karger, Basel, Switzerland.
15. **Callanan, J. J., B. A. Jones, J. Irvine, B. J. Willett, I. A. P. McCandlish, and O. Jarrett.** 1996. Histological classification and immunophenotype of lymphosarcomas in cats with naturally and experimentally acquired feline immunodeficiency virus infections. Vet. Pathol. **33:**264–272.
16. **Chakrabarti, L., M. Hurtrel, M.-A. Marie, R. Vazeux, D. Dormont, L. Montagnier, and B. Hurtrel.** 1991. Early viral replication in the brain of SIV-infected rhesus monkeys. Am. J. Pathol. **139:**1273–1280.
17. **Cinque, P., L. Vago, D. Ceresa, F. Mainini, M. R. Terreni, A. Vagani, W. Torri, S. Bossolasco, and A. Lazzarin.** 1998. Cerebrospinal fluid HIV-1 RNA levels: correlation with HIV encephalitis. AIDS **12:**389–394.
18. **Clements, J. E., T. Babas, J. L. Mankowski, K. Suryanarayana, M. Piatak, Jr., P. M. Tarwater, J. D. Lifson and M. C. Zink.** 2002. The central nervous system as a reservoir for simian immunodeficiency virus (SIV): steady-state levels of SIV DNA in brain from acute through asymptomatic infection. J. Infect. Dis. **186:**905–913.
19. **Cooper, D. A., J. Gold, P. Maclean, B. Donovan, R. Finlayson, T. G. Barnes, H. M. Michelmore, P. Brook, and R. Penny.** 1985. Definition of a clinical illness associated with seroconversion. Lancet **i:**537–540.
20. **Demuth, M., S. Czub, U. Sauer, E. Koutsilieri, P. ten Haaft, J. Heeney, C. Stahl-Hennig, V. ter Meulen, and S. Sopper.** 2000. Relationship between viral load in blood, cerebrospinal fluid, brain tissue and isolated microglia with neurological disease in macaques infected with different strains of SIV. J. Neurovirol. **6:**187–210.
21. **Désiré, N., A. Dehée, V. Schneider, C. Jacomet, C. Goujon, P.-M. Girard, W. Rozenbaum, and J.-C. Nicolas.** 2001. Quantification of human immunodeficiency virus type 1 proviral load by a taqman real-time PCR assay. J. Clin. Microbiol. **39:**1303–1310.
22. **Diehl, L. J., C. K. Mathiason-DuBard, L. L. O'Neil, and E. Hoover.** 1995. Longitudinal assessment of feline immunodeficiency virus kinetics in plasma by use of a quantitative competitive reverse transcriptase PCR. J. Virol. **69:**2328–2332.
23. **Diop, O. M., A. Gueye, M. Dias-Tavares, C. Kornfeld, A. Faye, P. Ave, M. Huerre, S. Corbet, F. Barre-Sinoussi, and M. C. Müller-Trutwin.** 2002. High levels of viral replication during the primary simian immunodeficiency virus SIVagm infection are rapidly and strongly controlled in African green monkeys. J. Virol. **74:**7538–7547.
24. **Di Stefano, M., L. Monno, J. R. Fiore, G. Buccoliero, A. Appice, L. M. Perulli, G. Pastore, and G. Angarano.** 1998. Neurological disorders during HIV-1 infection correlate with viral load in cerebrospinal fluid but not with virus phenotype. AIDS **12:**737–743.
25. **Dow, S. W., M. L. Poss, and E. A. Hoover.** 1990. Feline immunodeficiency virus: a neurotropic lentivirus. J. Acquir. Immune Defic. Syndr. **3:**658–668.
26. **Dow, S. W., M. J. Dreitz, and E. A. Hoover.** 1992. Feline immunodeficiency virus neurotropism. Evidence that astrocytes and microglial cells are the primary target cells. Vet. Immunol. Immunopathol. **35:**23–35.
27. **Flynn, J. N., C. A. Cannon, C. E. Lawrence, and O. Jarrett.** 1994. Polyclonal B-cell activation in cats infected with feline immunodeficiency virus. Immunology **81:**626–630.
28. **Gardner, M. B., and P. A. Luciw.** 1989. Animal models of AIDS. FASEB J. **3:**2593–2606.
29. **Gray, F., F. Scaravilli, I. Everall, F. Chretien, S. An, D. Boche, H. Adle-Biassette, L. Wingertsmann, M. Durigon, B. Hurtrel, F. Chiodi, J. Bell, and P. Lantos.** 1996. Neuropathology of early HIV-1 infection. Brain Pathol. **6:**1–15.
30. **Hofmann-Lehmann, R., R. K. Swenerton, V. Liska, C. M. Leutenegger, H. Lutz, H. M. McClure, and R. M. Ruprecht.** 2000. Sensitive and robust one-tube real-time reverse transcriptase-polymerase chain reaction to quantify SIV RNA load: comparison of one-versus two-enzyme systems. AIDS Res. Hum. Retrovir. **16:**1247–1257.
31. **Holzammar, S., E. Holznagel, A. Kaul, R. Kurth, and S. Norley.** 2001. High virus loads in naturally and experimentally SIVagm-infected African green monkeys. Virology **283:**324–331.
32. **Hosie, M. J., and O. Jarrett.** 1990. Serological responses of cats to feline immunodeficiency virus. AIDS **4:**215–220.
33. **Hosie, M. J., B. Willett, T. Dunsford, O. Jarrett, and J. C. Neil.** 1993. A monoclonal antibody which blocks infection with feline immunodeficiency virus identifies a possible non-CD4 receptor. J. Virol. **67:**1667–1671.
34. **Hosie, M. J., R. Osborne, J. K. Yamamoto, J. C. Neil, and O. Jarrett.** 1995. Protection against homologous but not heterologous challenge induced by inactivated feline immunodeficiency virus vaccines. J. Virol. **69:**1253–1255.
35. **Hosie, M. J., T. Dunsford, D. Klein, B. J. Willett, C. Cannon, R. Osborne, J. MacDonald, N. Spibey, N. Mackay, O. Jarrett, and J. C. Neil.** 2000. Vaccination with inactivated virus but not viral DNA reduces virus load following challenge with a heterologous and virulent isolated of feline immunodeficiency virus. J. Virol. **74:**9403–9411.
36. **Hosie, M. J., B. J. Willett, D. Klein, T. H. Dunsford, C. Cannon, M. Shimojima, J. C. Neil, and O. Jarrett.** 2002. Evolution of replication efficiency following infection with molecularly cloned feline immunodeficiency virus of low virulence. J. Virol. **76:**6062–6972.
37. **Hurtrel, B., L. Chakrabarti, M. Hurtrel, M.-A. Maire, D. Dormont, and L. Montagnier.** 1991. Early SIV encephalopathy. J. Med. Primatol. **20:**159–166.
38. **Hurtrel, M., J.-P. Ganière, J.-F. Guelfi, L. Chakrabarti, M.-A. Maire, F. Gray, L. Montagnier, and B. Hurtrel.** 1992. Comparison of early and late feline immunodeficiency virus encephalopathies. AIDS **6:**399–406.
39. **Ishida, T., and I. Tomoda.** 1990. Clinical staging of feline immunodeficiency virus infection. Jpn. J. Vet. Sci. **52:**645–648.
40. **Johnson, R. T., J. C. McArthur, and O. Narayan.** 1988. The neurobiology of human immunodeficiency virus infections. FASEB J. **2:**2970–2981.
41. **Klein, D., P. Janda, R. Steinborn, M. Muller, B. Salmons, and W. H. Günzburg.** 1999. Proviral load determination of different feline immunodeficiency virus isolates using real-time polymerase chain reaction: influence of mismatches on quantification. Electrophoresis **20:**291–299.
42. **Klein, D., B. Bugl, W. H. Günzburg, and B. Salmons.** 2000. Accurate estimation of transduction efficiency necessitates a multiplex real-time PCR. Gene Ther. **7:**458–463.
43. **Klein, D., C. M. Leutenegger, C. Bahula, P. Gold, R. Hofmann-Lehmann, B. Salmons, H. Lutz, and W. H. Günzburg.** 2001. Influence of preassay and sequence variations on viral load determination by a multiplex real-time reverse transcriptase-polymerase chain reaction for feline immunodeficiency virus. J. Acquir. Immune. Defic. Syndr. **26:**8–20.
44. **Leuteneggar, C., D. Klein, R. Hofmann-Lehmann, C. Mislin, U. Hummel, J. Boni, F. Boretti, W. Günzberg, and H. Lutz.** 1999. Rapid feline immunodeficiency virus provirus quantification by polymerase chain reaction using Taqman fluorogenic real-time detection system. J. Virol. Methods **78:**105–116.
45. **Leutenegger, C. M., J. Higgins, T. B. Matthews, A. F. Tarantal, P. A. Luciw, N. C. Pederseon, and T. W. North.** 2001. Real-time TaqMan PCR as a specific and more sensitive alternative to the branched-chain DNA assay for quantification of simian immunodeficiency virus RNA. AIDS Res. Hum. Retrovir. **17:**243–251.
46. **McArthur, J. C., D. R. McClernon, M. F. Cronin, T. E. Nance-Sproson, A. J. Saa, M. St. Clair, and E. R. Lanier.** 1997. Relationship between human immunodeficiency virus-associated dementia and viral load in cerebrospinal fluid and brain. Ann. Neurol **42:**675–678.
47. **Overbaugh, J., P. A. Luciw, and E. A. Hoover.** 1997. Models for AIDS

pathogenesis: simian immunodeficiency virus, simian-human immunodeficiency virus and feline immunodeficiency virus infections. AIDS **11:**S47–S54.
48. **Pedersen, N. C., E. W. Ho, M. L. Brown, and J. K. Yamamoto.** 1987. Isolation of a T-lymphotropic virus from domestic cats with an immunodeficiency like syndrome. Science **235:**790–793.
49. **Pedersen, N. C., J. K. Yamamoto, T. Ishida, and H. Hansen.** 1989. Feline immunodeficiency virus infection. Vet Immunol. Immunopathol. **21:**229–243.
50. **Pedersen, N. C., and J. E. Barlough.** 1991. Clinical overview of feline immunodeficiency virus. J. Am. Vet. Med. Assoc. **199:**1298–1305.
51. **Pedersen, N. C., C. M. Leuteneggar, J. Woo, and J. Higgins.** 2001. Virulence difference between two field isolates of feline immunodeficiency virus (FIV-Apetaluma and FIV-Cpgammar) in young adult specific pathogen free cats. Vet. Immunol. Immunopathol. **79:**53–67.
52. **Persidsky, Y., H. S. Nottet, V. G. Sasserville, L. G. Epstein, and H. E. Gendelman.** 1995. The development of animal model systems for HIV-1 encephalitis and its associated dementia. J. Neurovirol. **1:**229–243.
53. **Piatak, M., Jr., M. S. Saag, L. C. Yang, S. J. Clark, J. C. Kappes, K.-C. Luk, B. H. Hahn, G. M. Shaw, and J. D. Lifson.** 1993. High levels of HIV-1 in plasma during all stages of infection determined by competitive PCR. Science **259:**1749–1754.
54. **Pistello, M., S. Menzo, M. Giorgi, L. Da Prato, G. Cammarota, M. Clementi, and M. Bendinelli.** 1994. Competitive polymerase chain reaction for quantitating feline immunodeficiency virus load in infected cat tissues. Mol. Cell. Probes **8:**229–234.
55. **Podell, M., M. Oglesbee, L. Mathes, S. Krakowka, R. Olmstead, and L. Lafrado.** 1993. AIDS-associated encephalopathy with experimental feline immunodeficiency virus infection. J. Acquir. Immune. Defic. Syndr. **6:**758–771.
56. **Podell, M., K. Hayes, M. Oglesbee, and L. Mathes.** 1997. Progressive encephalopathy associated with CD4/CD8 inversion in adult FIV-infected cats. J. Acquir. Immune Defic. Syndr. Hum. Retrovirol. **15:**332–340.
57. **Podell, M., P. A. March, W. R. Buck, and L. E. Mathes.** 2000. The feline model of neuroAIDS: understanding the progression towards AIDS dementia. J. Psychopharmacol. **14:**205–213.
58. **Poli, A., M. Pistello, M. A. Carli, F. Abramo, G. Mancuso, E. Nicoletti, and M. Bendinelli.** 1999. Tumour necrosis factor-α and virus expression in the central nervous system of cats infected with feline immunodeficiency virus. J. Neurovirol. **5:**465–473.
59. **Pomerantz, R. J.** 2002. Reservoirs of human immunodeficiency virus type-1: the main obstacles to viral eradication. Clin. Infect. Dis. **34:**91–97.
60. **Schutten, M., B. van den Hoogan, M. E. van der Ende, R. A. Gruters, A. D. Osterhaus, and H. G. Niesters.** 2000. Development of a real-time quantitative RT-PCR for the detection of HIV-2 RNA in plasma. J. Virol. Methods **88:**81–87.
61. **Suryanarayana, K., T. A. Wiltrout, G. M. Vasquez, V. M. Hirsch, and J. D. Lifson.** 1998. Plasma SIV RNA viral load determination by real-time quantification of product generation in reverse transcriptase-polymerase chain reaction. AIDS Res. Hum. Retrovir. **14:**183–189.
62. **Vahlenkamp, T. W., H. F. Egberink, M. J. T. van Eijl, A. M. E. Slotboom-Kamphorst, E. J. Verschoor, M. C. Horzinek, and A. de Ronde.** 1995. Competitive reverse transcription-polymerase chain reaction for quantification of feline immunodeficiency virus. J. Virol. Methods **52:**335–346.
63. **Wiley, C. A., V. Sootornniyomkij, L. Radhakrishnan, E. Masliah, J. Mellors, S. A. Hermann, P. Dailey, and C. L. Achim.** 1998. Distribution of brain HIV load in AIDS. Brain Pathol. **8:**227–284.
64. **Willett, B. J., M. J. Hosie, J. J. Callanan, J. C. Neil, and O. Jarrett.** 1993. Infection with feline immunodeficiency virus is followed by the rapid expansion of a CD8+ lymphocyte subset. Immunology **78:**1–6.
65. **Willett, B. J., J. N. Flynn, and M. J. Hosie.** 1997. FIV infection of the domestic cat: an animal model for AIDS. Immunol. Today **18:**182–189.
66. **Willett, B. J., L. Picard, M. J. Hosie, L. D. Turner, K. Adema, and P. R. Claphman.** 1997. Shared usage of the chemokine receptor CXCR4 by the feline and human immunodeficiency viruses. J. Virol. **71:**6407–6415.
67. **Yamamoto, J. K., E. Sparger, E. W. Ho, P. R. Andersen, T. P. O'Connor, C. P. Mandell, L. Lowenstine, R. Munn, and N. C. Pedersen.** 1988. Pathogenesis of experimentally induced feline immunodeficiency virus infection in cats. Am. J. Vet. Res. **8:**1246–1258.
68. **Zink, M. C., K. Suryanarayana, J. Mankowski, A. Shen, M. Piatak, Jr., J. P. Spelman, D. L. Carter, R. J. Adams, J. D. Lifson, and J. E. Clements.** 1999. High viral load in the cerebrospinal fluid and brain correlates with severity of simian immunodeficiency virus encephalitis. J. Virol. **73:**10480–10488.